32

Adaptive Calibration and Quality Control of Smart Sensors

Matej Možek, Danilo Vrtačnik, Drago Resnik,
Borut Pečar and Slavko Amon
Laboratory of Microsensor Structures and Electronics (LMSE)
Faculty of Electrical Engineering, University of Ljubljana
Tržaška 25, Ljubljana,
Slovenia

1. Introduction

Smart sensors represent an attractive approach in sensor applications due to their adaptability, achieved by means of digital signal processing. Sensor adaptability can be further turned into a major advantage by introduction of smart calibration systems.
Smart sensors are generally integrated with signal conditioning circuits. Signal conditioning circuits are needed to adjust the offset voltage and span, for compensation of temperature effects of both offset voltage and span, as well as to provide an appropriately amplified signal. The proposed approach is based on a special case of smart pressure sensors, but the developed calibration system is generally applicable for any kind of smart sensor.
In manufacturing of modern electronic devices achieving and maintaining high yield level is a challenging task, depending primarily on the capability of identifying and correcting repetitive failure mechanisms. Yield enhancement is defined as the process of improving the baseline yield for a given technology generation from R&D yield level to mature yield. Yield enhancement is one of the strategic topics of ITRS (International Technology Roadmap for Semiconductors, Test And Test Equipment, 2006). This iterative improvement of yield is based on yield learning process, which is a collection and application of knowledge of manufacturing process in order to improve device yield through the identification and resolution of systematic and random manufacturing events (International Technology Roadmap for Semiconductors, Yield Enhancement, 2006). Yield improvement process will consequentially increase the number of test parameters and hence the calibration system complexity. One of advantages of increasing system complexity is the ability to integrate the input testing processes and output final testing processes into the calibration process itself, thus shortening the total time for calibration.
Several types of smart sensors with integrated signal conditioning have been presented over the past few years (Takashima et al., 1997) & (IEEE Std. 1451.2 D3.05, 1997). The calibration processes and temperature compensating methods for these sensors are based either on analog, digital or mixed approaches. Analog approach usually comprises an amplifier with laser trimmable thin film resistors (Chau et al., 1997) & (Wang et al., 2005) or off-chip trimmable potentiometers (Schnatz et al., 1992) & (Lee et al., 1999), to calibrate the sensor span and offset voltage and to compensate for their temperature drift. Analog compensation

techniques are relatively slow, inflexible and cost-ineffective. In digital approach, sampling for raw digital pressure and temperature values is first performed, followed by an evaluation of the output digital values via polynomials for describing sensor characteristic, and finally converting the computed pressure values to according analog voltages (ZMD31020 description, 2002) & (ZMD31050 description, 2005). Mixed approach retains strictly the analog signal conversion path, while smart sensor offset and span are adjusted by setting of operational amplifiers by digital means (MLX90269 datasheet, 2006).
This paper will focus on the problem of adaptive calibration any quality control of smart sensors with digital temperature compensation, which is one of the most time consuming steps in sensor production. In order to advance calibration system performance, smart calibration system is conceived as a digitally controlled closed loop system capable of adaptive learning. Presented concept of calibration system is directly implemented in the iterative yield enhancement process in the production of piezoresistive pressure sensors for automotive applications. The calibration system operation and quality control is illustrated on the case of Manifold Absolute Pressure (MAP) sensors. The emphasis will be on MAP sensors, although the proposed approach can be implemented in other fields of application.

2. Calibration procedure

Main calibration procedure starts with measurement of sensor coarse gain and offset and optimization of sensor parameters to the sensor signal conditioner front end stage. After initial optimization procedure the calibration conditions are set according to calibration scenario. Raw sensor readouts of supplied reference quantities are acquired at each calibration point. After acquisition, digital description of sensor characteristic is evaluated and the results are stored back to sensor. A detailed description of calibration procedure is given in (Možek et al., 2008). Calibration scenario defines the sequence of reference quantities, which are applied to sensors under calibration. In case of temperature compensation of pressure sensor, the reference quantities are pressure and temperature. Minimal number of calibration points is 4. This is defined by using the lowest (i.e. linear) degree of polynomial for sensor characteristic description (ZMD31020 description, 2002) & (ZMD31050 description, 2005) in the temperature and pressure direction.
The calculation function used in the ZMD31020 signal conditioner is given in equation (1). It covers variations in sensor offset, sensitivity and first order nonlinearity.

$$p = 2^{12}\frac{2^{2}\cdot p_{oc} + 2^{-24}\cdot a_0\cdot p^{2}_{oc} + a_1 + 2^{-9}\cdot a_2\cdot\left(T_{oc}-550\right) + 2^{-18}\cdot a_3\cdot\left(T_{oc}-550\right)^{2}}{a_4 + 2^{-9}\cdot a_5\cdot\left(T_{oc}-550\right) + 2^{-18}\cdot a_6\cdot\left(T_{oc}-550\right)^{2}} \tag{1}$$

where p is the resulting corrected sensor signal, p_{oc} is an uncorrected raw analog to digital converter readout from pressure sensor, T_{oc} is a offset corrected raw analog to digital converter readout from temperature sensor and a_0 through a_6 are calibration coefficients of pressure sensor.
Maximal number of calibration points is primarily limited by total calibration time. In case of pressure sensors, both calibration axes consist of three calibration points, thus enabling compensation of second order nonlinearity in both directions, as depicted in Fig. 1.
Maximal number of calibration points for pressure sensor can cover nonlinearities up to third order in pressure direction. Actual number of calibration points is a compromise between calibration precision and total calibration time. To shorten total calibration time,

the slower settling axis should be used for definition of the calibration points order. In case of MAP sensor, the temperature axis defines the calibration scenario.

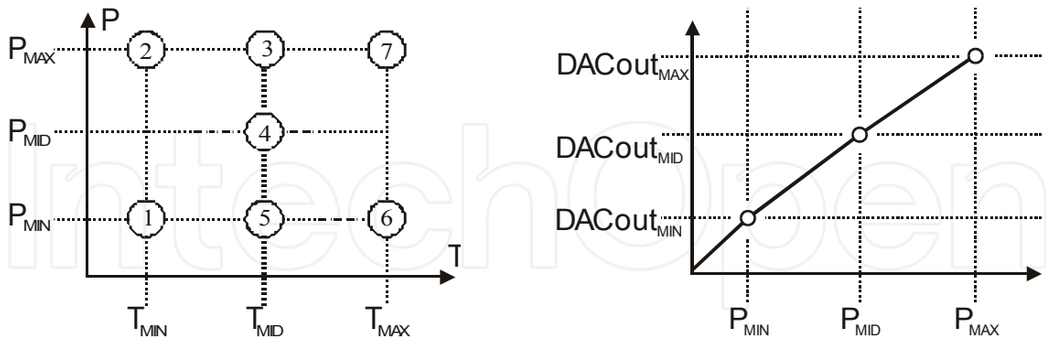

Fig. 1. Calibration scenario

2.1 Sensor range optimization

Optimization algorithms are varying the signal conditioner front-end parameters in order to fit sensor response variations into desired analog to digital converter measurement range. The ZMD31020 preamplifier features three settings of preamplifier gain (15.66, 24 or 42). The preamplifier gain settings cover a wide sensor sensitivity range. The corresponding value of gain is found by altering the gain setting at full scale pressure applied in calibration point 2 of the calibration scenario. Note, that gain optimization is performed at minimal temperature, due to negative temperature coefficient of pressure sensor sensitivity. The signal conditioner readout is evaluated at each setting. If the signal conditioner readout exceeds the limit of maximal readout available (4095), the value of signal conditioner gain must be lowered. Maximal gain, which complies with gain optimization criterion, is selected. For relative pressure sensors, both negative and positive full-scale signal conditioner responses must be evaluated for each gain setting. Maximal gain, which complies with signal conditioner limits for both pressure values, is selected. Output reference bias (zero signal response of pressure analog to digital converter) can be offset to either 1/16, 1/8, 1/4 or 1/2 of analog to digital converter measurement range (0...4095). In case of relative pressure sensors, the value of digital range shift (CRROB) is usually fixed at 1/2, since the measurement range should be centered. In case of absolute pressure sensor, the range shifting is performed at calibration point 1. Sensor zero scale response is read and the values are evaluated. The values are compared to zero response. If the output is clamped to zero, higher range shift option is selected. The selected option represents the minimal value of range shift. Measurement and acquisition of raw data is normally a two stage process described in equation (2) for temperature measurement.

$$T_1 = 2^{10}\left[\frac{V_{offsetT}[V]}{0.98V} + \frac{1}{16}\right] \quad T_2 = 2^{10}\left[\frac{V_{temp}[V] + V_{offsetT}[V]}{0.98V} + \frac{1}{16}\right]$$
$$T_{OC} = T_2 - T_1 = 2^{10}\frac{V_{temp}[V]}{0.98V} \tag{2}$$

where $V_{offsetT}$ is the offset voltage of the temperature sensor measurement path, V_{temp} is the signal from temperature sensor and T_{OC} is the offset corrected value of temperature sensor

readout. Addition factor of 1/16 represents the value of corresponding bias voltage, used to adapt the temperature analog to digital converter conversion range. The voltage 0.98 V is the differential temperature analog to digital converter reference voltage. Similarly, the pressure measurement process is a two stage process described by equation (3).

$$P_1 = 2^{12}\left[\frac{A \cdot V_{offsetP}}{0.98 \cdot V_{REF}} + CRROB\right] \quad P_2 = 2^{12}\left[\frac{A \cdot \left(V_{pressure} + V_{offsetP}\right)}{0.98 \cdot V_{REF}} + CRROB\right]$$
$$P_{OC} = P_2 - P_1 = 2^{12}\frac{A \cdot V_{pressure}}{0.98 \cdot V_{REF}} \tag{3}$$

where $V_{offsetP}$ is the offset voltage of the pressure sensor measurement path, $V_{pressure}$ is the signal from pressure sensor and P_{OC} is the offset corrected value of pressure sensor readout. Addition factor of CRROB represents the value of conversion range referenced output bias, used to adapt the pressure analog to digital converter conversion range to different sensor applications (absolute, relative). The voltage $0.98V_{REF}$ is the differential ratiometric analog to digital converter reference voltage. The conversion stage can be supplied by arbitrary V_{REF} voltage within [V_{SS}...V_{DD}] limits. Normally, the value equals V_{DD}. Voltage V_{REF} can be derived from supply voltage, thus making the conversion full ratiometric.

2.2 Acquisition of raw pressure and temperature readout

The readouts from pressure and temperature acquisition are gathered by the calibration station. The calibration station also controls the stability of calibration point conditions. The major advantage of digital calibration system is that stability of a reference pressure and temperature can be controlled by using the sensors being calibrated. The latter becomes effective in case of temperature stabilization, where temperature stability of ΔT=0.2 °C must be assured within calibration chamber. Such temperature stability would normally require an expensive temperature chamber, which still would not solve the problem of temperature stability on the sensors themselves. The same applies for reference pressure value. In order to achieve the most stable reference conditions on the sensors, raw pressure and temperature sensor response have to be filtered. This is performed by means of digital implementation of moving average low-pass filter as depicted in Fig. 2..

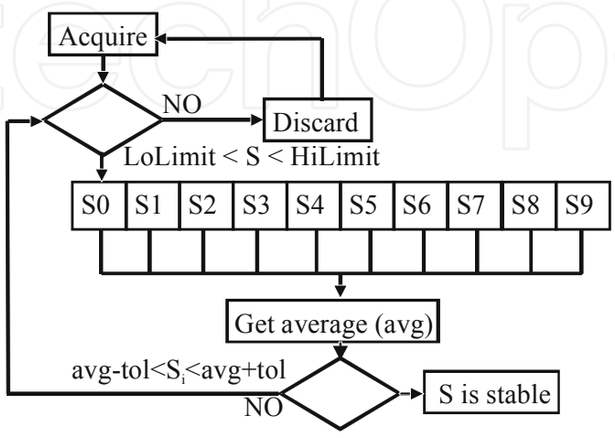

Fig. 2. Moving average filter algorithm for pressure and temperature acquisition

The input sample is first checked for valid limits. If it complies with preset limits, it enters the moving average filter loop. The sampling continues and the complying measured samples are stored in the filter array. At every measurement, filter average is calculated, and the resulting filter average is compared to every sample (S_i) residing in the filter array. The tolerance from current filter average (noted as *tol* in Fig. 2) is used to determine the level of residual measurement noise. This parameter is set in the calibration system setup according to acquisition noise level during calibration. The value of filter tolerance (ε) is calculated in percent of full scale response.

$$\varepsilon = \frac{tol}{2^{RADC}} \cdot 100\% \tag{4}$$

For typical application, where R_{ADC}=13 bits, filter tolerance is 0.06 %FS. The amount of acquisition noise, filtered by such moving average filter can be minimized by either lowering the tolerance parameter or by increasing the filter length.
Filter lengths are different for temperature and pressure acquisition. For pressure sampling point acquisition, ten filter elements have proven to be enough for system noise minimization according to described system setup. On the other hand, for temperature setpoint, filter length is 60 elements, and additional sampling delay of 1 s was introduced. Increasing the filter length also increases the filter stabilization time – i.e. filter step response, hence a compromise between noise level filtering and step response time must be achieved. Both finite and infinite impulse response filter implementations (FIR, IIR) were tested. Equation (5) represents the IIR realization of moving average low-pass filter, while the FIR representation is given in equation (6).

$$y_n = \frac{x_n - x_{n-N}}{N} + y_{n-1} \tag{5}$$

$$y_n = \frac{x_n + x_{n-1} + x_{n-2} + \ldots x_{n-(N-1)}}{N} \tag{6}$$

IIR filter realizations are, although simpler to evaluate, inappropriate due to their instability and non-linear phase response. Stability and linear filter phase response are prerequisite for such application as sensor noise filtering, because they offer instant information about stabilization of measurement quantity.

2.3 Calibration of signal-conditioner analog output stage

This step was introduced after the initial version of ZMD31020 calibration system was completed. During the initial calibrations of sensors with analog output, a large output voltage error of calibrated sensors was noticed. This error was attributed to temperature dependency and chip-to-chip differences of output digital to analog converter characteristic. After the raw pressure and temperature sensor output have been measured at a given calibration point, the sensor analog output digital to analog converter has to be set to match the desired voltage response at a given calibration point. Signal conditioner 11 bit digital to analog converter response exhibits large chip-to-chip differences as shown in Fig. 3. In Fig. 3 the digital to analog converter digital setting histogram at calibration point 5 is shown at a calibration point of 17 kPa and temperature 35 °C. Calibration results based on 36049 sensors are depicted in the Fig. 3.

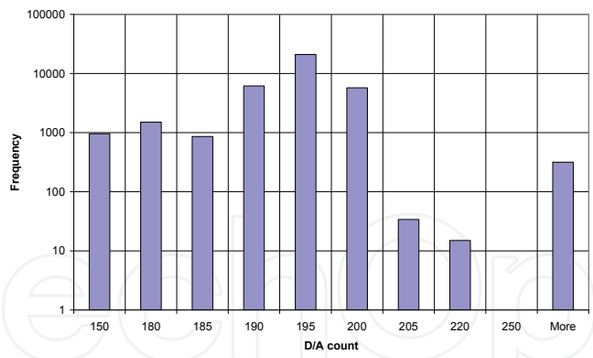

Fig. 3. Digital to analog converter readout at calibration point 5 of calibration scenario

At a given point, the desired sensor output should be at 0.25 V at a power supply voltage of 5 V, so the corresponding ideal linear digital to analog converter setting would be at 205 counts.

$$DAC = \frac{0.25V}{5V} \cdot (2^{12} - 1) = 205 \tag{7}$$

However, if this calculated value is fed into calculation of calibration coefficients, the sensor output actually varies from ideal value. The results show that most signal conditioners don't comply with the calculated ideal value of 205 counts and furthermore there may be large variations (up to 50 digital to analog converter levels) from this ideal value.

One reason for variations is the output stage itself: The signal conditioner digital to analog converter characteristic is described with no load on the sensor output, however this is not the case in real-world sensor application. The signal conditioner namely "features" a rather poor output current driving capability, which is deteriorated by introducing additional pull-up resistance on the sensor output. Second reason lies in the technological chip-to-chip variations of digital to analog converter.

In order to produce an accurate analog output signal, these variations must be compensated. The adjustment of sensor analog output is performed by iterative algorithms, based on successive approximation (SA) principle or P regulator principle. The sensor analog output calibration mechanism provides means for minimization of system specific errors (e.g. calibration point to calibration point errors) as well as sensor specific errors (e.g. signal conditioner chip to chip errors). The digital to analog converter calibration mechanism is based on the successive approximation method, where every sensor digital to analog converter output is measured by a 40 channel data acquisition (DAQ) system. Sensors are also connected to a host computer via digital interface. This arrangement of instruments forms a closed regulation loop which adjusts the sensor digital to analog converter output according to successive approximation algorithm in such a manner that the desired output response (V_{SET}) is obtained at every temperature of calibration. The register of the sensor output digital to analog converter (DAC_{OUT}) can be set according to successive approximation method. The digital to analog converter response voltage (V_{DAC}) is measured and compared to desired output response (V_{SET}). If the V_{DAC} value exceeds the V_{SET} voltage, the preset DAC_{OUT} bit has to be set to zero, or it remains set to one. Algorithm starts with MSB (most significant bit) and has to be iterated 11 times, which equals the number of digital to analog converter bits. The process is time-consuming, especially if output voltage

scanning is performed upon 128 or more sensors. Instead of calibrating the digital to analog converter via successive approximation principle, a novel P regulator based calibration mechanism was introduced. This principle shortens the number of iterations from initial 11 to typically 2 or 3 iterations. Initially, the digital to analog converter register value DAC_{OUT} is calculated according to "ideal" digital to analog converter transfer characteristics:

$$DAC_{OUT} = \frac{V_{\text{supply}}}{2^{11}} \cdot V_{SET} \tag{8}$$

The initial value covers two variables during digital to analog converter calibration. First one is the supply voltage variation, which is "ideally" considered to be 5 V, and the second one are chip-to-chip variations of the digital value of digital to analog converter. The supply voltage has to be measured before any corrections are made to the digital to analog converter output. The digital to analog converter register value is transmitted to the sensor and the corresponding output voltage V_{OUT} is set. The V_{OUT} voltage is then measured and error is calculated as a difference between calibration point digital to analog converter set value V_{SET} and the measured voltage V_{OUT}. This voltage error is converted to digital value by multiplying with 2^{11} and the resulting digital error value is added to digital representation of digital to analog converter voltage. The loop is iterating until the error becomes less than 0.5 LSB (least significant bit). The exit criterion was chosen to be <0.5 LSB, so that LSB is also set for minimal V_{OUT} error.

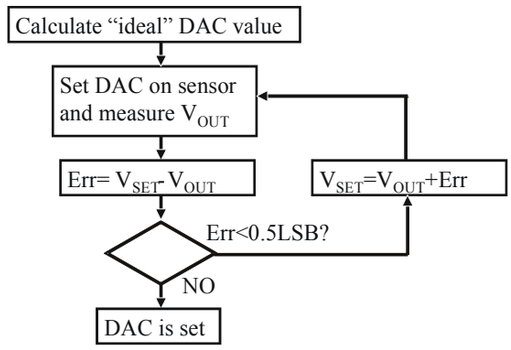

Fig. 4. P regulator based digital to analog converter calibration flow diagram

This algorithm can be executed either on sensors with ratiometric voltage output or fixed voltage output.

2.4 Calibration coefficients calculation

A set of seven coefficients (a_0 ... a_6) must be evaluated in order to take full advantage of calculation precision of sensor characteristic description, expressed in equation (1). Maximal number of acquired data points is limited to seven. Equation (1), which defines the ZMD31020 sensor characteristic, contains only non-involuted coefficients, enabling simple computation of unknown sensor coefficients. If the equation (1) is arranged into form (9) we obtain

$$\begin{aligned} &-2^{-12} \cdot P_{OC}^2 \cdot a_0 - 2^{12} \cdot a_1 - 2^3 \cdot T_{OC} \cdot a_2 - 2^{-6} \cdot {T_{OC}}^2 \cdot a_3 + p \cdot a_4 \ldots \\ &\ldots - 2^{-9} \cdot p \cdot T_{OC} \cdot a_5 - 2^{-18} \cdot p \cdot T_{OC}^2 \cdot a_6 = 2^{14} \cdot P_{OC} \end{aligned} \tag{9}$$

If seven acquired calibration points are numbered $CP_1..CP_7$, each CP_X having its corresponding raw pressure and temperature output and desired output (P_{OCX}, T_{OCX}, and p_X respectively), the coefficients can be determined by resolving a linear system of seven equations:

$$[C]\cdot[A]=[P]$$

$$C=\begin{bmatrix} -2^{-12}\cdot P_{OC1}^2 & -2^{12} & -2^3\cdot T_{OC1} & -2^{-6}\cdot T_{OC1}{}^2 & p_1 & -2^{-9}\cdot p_1\cdot T_{OC1} & -2^{-18}\cdot p_1\cdot T_{OC1}^2 \\ -2^{-12}\cdot P_{OC2}^2 & -2^{12} & -2^3\cdot T_{OC2} & -2^{-6}\cdot T_{OC2}{}^2 & p_2 & -2^{-9}\cdot p_2\cdot T_{OC2} & -2^{-18}\cdot p_2\cdot T_{OC2}^2 \\ -2^{-12}\cdot P_{OC3}^2 & -2^{12} & -2^3\cdot T_{OC3} & -2^{-6}\cdot T_{OC3}{}^2 & p_3 & -2^{-9}\cdot p_3\cdot T_{OC3} & -2^{-18}\cdot p_3\cdot T_{OC3}^2 \\ -2^{-12}\cdot P_{OC4}^2 & -2^{12} & -2^3\cdot T_{OC4} & -2^{-6}\cdot T_{OC4}{}^2 & p_4 & -2^{-9}\cdot p_4\cdot T_{OC4} & -2^{-18}\cdot p_4\cdot T_{OC4}^2 \\ -2^{-12}\cdot P_{OC5}^2 & -2^{12} & -2^3\cdot T_{OC5} & -2^{-6}\cdot T_{OC5}{}^2 & p_5 & -2^{-9}\cdot p_5\cdot T_{OC5} & -2^{-18}\cdot p_5\cdot T_{OC5}^2 \\ -2^{-12}\cdot P_{OC6}^2 & -2^{12} & -2^3\cdot T_{OC6} & -2^{-6}\cdot T_{OC6}{}^2 & p_6 & -2^{-9}\cdot p_6\cdot T_{OC6} & -2^{-18}\cdot p_6\cdot T_{OC6}^2 \\ -2^{-12}\cdot P_{OC7}^2 & -2^{12} & -2^3\cdot T_{OC7} & -2^{-6}\cdot T_{OC7}{}^2 & p_7 & -2^{-9}\cdot p_7\cdot T_{OC7} & -2^{-18}\cdot p_7\cdot T_{OC7}^2 \end{bmatrix} \quad (10)$$

$$A=\begin{bmatrix} a_0 & a_1 & a_2 & a_3 & a_4 & a_5 & a_6 \end{bmatrix}^T$$

$$P=\begin{bmatrix} 2^{14}\cdot P_{OC1} & 2^{14}\cdot P_{OC2} & 2^{14}\cdot P_{OC3} & 2^{14}\cdot P_{OC4} & 2^{14}\cdot P_{OC5} & 2^{14}\cdot P_{OC6} & 2^{14}\cdot P_{OC7} \end{bmatrix}^T$$

where [C] represents a calibration point matrix, [A] an unknown coefficient vector and P represents pressure values from calibration points. The most prevalent Gaussian elimination was implemented into the calibration system. However, as the calculation of calibration coefficients is well known procedure, care must be taken when deciding upon the final set of coefficients. The computation of linear system of equations is performed using floating point calculations. Sensor correction microcontroller on the other hand is evaluating equations (2) and (3) using 16 bit integer arithmetic. In order to minimize the sensor calculation error, all coefficient rounding combinations have to be evaluated versus ideal (desired - p_x) sensor response at every calibration point. A dedicated algorithm for simulating actual sensor digital response by forcing 16-bit arithmetic was also implemented. Combinations of rounded coefficients (a_0 ... a_6) are subsequently inserted into implementation and normalized difference at ε_{CPi} between desired output $p_{DESIRED}$ and computer simulted output $p_{GetResult}$ evaluated at every calibration point.

$$\varepsilon_{CPi}=\left|\frac{p_{DESIRED}-p_{\text{GetResult}}}{p_{DESIRED}}\right|\cdot 100\% \quad \rightarrow \quad \varepsilon=\frac{1}{N}\sqrt{\sum_{i=1}^{N}\varepsilon_{CPi}^2} \quad (11)$$

where N denotes number of calibration points and ε_{CPi} denotes the calibration error at a given calibration point and ε denotes total calibration error. The normalization with square root of sum of squares was used to amplify large errors and make better distinction of faulty sensors.

2.5 Evaluation of parameters at calibration input

Calibration scenario enables the assessment of essential input parameters to calibration procedure, which enables early fault detection on sensors before they enter actual calibration process. Input parameters comprise the properties, such as offset, sensitivity and nonlinearity of uncompensated sensing element (e.g. pressure sensor). Evaluation of such properties is essential for determination of decision criteria for adaptive concept of calibration system.

Sensor sensitivity can be evaluated at three temperatures. At each temperature, sensitivity is obtained as a difference of pressure sensor voltage response, normalized to corresponding pressure change.

Temperature coefficient of pressure sensor sensitivity is evaluated as a difference between sensor sensitivities at two temperature endpoints (T_{MIN} and T_{MAX} in Fig. 1). Resulting difference is normalized to temperature corresponding temperature change. Sensor offset at room temperature can be evaluated at calibration point 5 as T_{MID} in Fig. 1 is normally set at room temperature. Digital sensor offset readout is transformed into voltage according to analog to digital ASIC stage parameters using equations (2) and (3).

Temperature coefficient of sensor offset is estimated from endpoint calibration points offset values normalized to corresponding temperature difference. In presented calibration scenario the calibration endpoints for estimation of temperature coefficient are marked 1 and 6. Obtained result is recalculated to temperature response at 0°C.

Nonlinearity is calculated by using calibration points 3, 4 and 5 in Fig. 1. Nonlinearity is evaluated as a difference of midpoint pressure response at calibration point 4 from ideal linear sensor response, formed by calibration points 3 and 5. Resulting difference is normalized to calibration span, defined by calibration points 3 and 5. For practical purposes, evaluation of sensor nonlinearity is performed only at room temperature.

Temperature sensor sensitivity in (mV/°C) is calculated by evaluation of raw temperature sensor response difference according to (2) in calibration scenario (Fig. 1) between calibration points 1 and 6. Similar response difference can be obtained from calibration points 2 and 7. Evaluated sensitivities are stored in the calibration database as parameter TCSx, where x denotes the number of calibration point.

Temperature sensor nonlinearity is calculated by evaluation of raw temperature response difference according to equation (2) in calibration scenario (Fig. 1) between calibration points 1, 5 and 6. Linear temperature sensor response is calculated between endpoints 1 and 6. The difference between calculated value at temperature T_{MID} (see Fig. 1) and actual readout from temperature sensor are normalized to previously calculated temperature sensor sensitivity on a corresponding calibration point. Resulting temperature nonlinearity stored in the calibration database as parameter TNLx, where x denotes the number of calibration point. Note, that temperature sensor nonlinearity cannot be evaluated at calibration point 4 according to calibration scenario in Fig. 1. Calculated nonlinearity has the same value for calibration points 1, 5 and 6 and calibration points 2, 3 and 7.

Temperature coefficient of offset is calculated after evaluation of sensor offset values at three temperatures in calibration scenario in Fig. 1. The temperature coefficient of offset is defined as a difference of previously obtained sensor offset values over a temperature interval, formed by temperature T_{MIN} and T_{MAX}. Resulting values from calculation are stored as parameter TCOFx, where x denotes the number of calibration point. Units are [µV/°C]. For applied calibration scenario, the TCOFx parameter value is the same for every calibration point. Temperature coefficient of sensitivity is calculated after evaluation of sensor sensitivities at a given temperature in calibration scenario. The temperature coefficient of sensitivity is defined as a difference of sensor sensitivity over a given temperature interval. The temperature coefficient of sensitivity is defined as a difference of previously obtained sensor sensitivity values over a temperature interval, formed by temperature T_{MIN} and T_{MAX}. Resulting values from calculation are stored as parameter TCSx, where x denotes the number of calibration point. Units are [(mV/V/bar)/°C]. For applied calibration scenario, the TCSx parameter value is the same for every calibration point.

2.6 Evaluation of parameters at calibration output

Calibration output parameters are directly related to compensation of unwanted dependencies. In case of presented MAP pressure sensor this is the temperature compensation. Temperature error is evaluated at every calibration point immediately after evaluation of calibration coefficients. It is calculated by calibration computer as a difference between output of ideal characteristic of MAP sensor and the ASIC simulation of sensor characteristic. Total temperature error comprises RSS (root square of sum of squares) of temperature errors, calculated at every calibration point. Total calibration error is comprised of RSS sum of total temperature error and the combined standard uncertainty for output analog stage, if the sensor features analog output. The ASIC features 16 bit integer arithmetic, therefore a rounding error, which occurs during coefficients calculation, is further minimized by evaluation of total temperature error on all rounding combinations. Rounding combination of calibration coefficients, that yields minimal temperature error at each calibration point is written to ASIC.

2.7 Sensor failure analysis

The analysis of acquired parameters can unveil several causes of sensor failure. Not all causes are universally implied by the large calibration error, therefore failure analysis must be performed on each calibrated sensor. The causes of failure can be either sensor related or system related. Furthermore, the sensor related failures can be divided into signal conditioner failures and sensing element (either pressure or temperature sensor) failure. Detailed detection of system related causes makes the calibration system itself smart.

Non-zero sensor error can be caused by inadequate raw pressure or temperature sensor response: The temperature is measured by an ASIC by measuring a voltage drop on internal diode or an external temperature sensing element (resistor, diode). The available voltage response on internal diode is predefined within interval [294 ... 805] counts for ZMD31020. First, the sensor temperature response is checked against these limits and the response is evaluated. If the sensor response doesn't comply with these limits, an error is raised and sensor is excluded from further evaluation. This error is related to ASIC failure or ASIC bonding failure. Furthermore, the temperature sensor response is also checked at different calibration temperatures – if the response stays within predefined limit, the temperature sensing element is clearly faulty.

2.8 ASIC response related causes of failure

Inadequate raw pressure sensor response is detected by comparing the sensor sensitivity response at a given temperature after successful range optimization was performed. Range optimization technique adapts the ASIC amplifier parameters so that sensor sensitivity should be adapted to analog to digital converter measurement range. Normal raw pressure sensor response difference between minimal and maximal pressure is therefore in the range of 2^R counts, where the R represents the analog to digital converter resolution. If the sensor sensitivity stays well below 2^R, then the sensor is considered faulty due to inadequate pressure response. The "well below 2^R" limit is set at a 3/4 of analog to digital converter measurement range. Calibration errors from ASIC can be related to faulty temperature sensor. The calibration setup was based on a temperature sensing element, located on the ASIC. Furthermore, electrical connection failure can be detected and calculation related

errors, which are caused by 16-bit arithmetic used in the ASIC. Electrical connections can fail on the ASIC side, which is immediately detected by the calibration system, because of digital interface error. If any of the sensor bonds fail, this error may be considered same as inadequate sensor response, because the sensor readout will be constant for different excitations. The main ASIC related cause of non-zero calibration error ε_{cpi} is related to calculation error. The arithmetic in ASIC is namely 16-bit, hence calibration coefficients must not exceed the integer value interval [-32678...32767]. Therefore a solution to the system of equations may exist, but the coefficients are clamped to either limit of validity interval, leading to erroneous digital output values.

2.9 Calibration system related causes of failure

Inadequate raw pressure sensor response can be also related to pressure controller failure. To distinguish between pressure leakage and inadequate raw pressure sensor response, a separate reference pressure sensor is connected to a pressure line and it constantly monitors the pressure. Moreover, if there is any leakage in the pressure connection, the controller will not stabilize and the calibration procedure stays put. The calibration system warns the operator for leakage, but finding an actual spot of leakage is still a human operator related issue.

Second major system failure can be related to temperature instability. As the temperature stabilization is achieved by sensors themselves, the temperature stability is checked versus all orthogonal calibration points in calibration scenario. If the temperature varies more than 10 counts over all orthogonal temperature points, a warning is raised due to unstable temperature conditions. Another cause of system failure is that the system fails to stabilize after predefined maximum temperature stabilization time. If temperature stabilization timeout is detected, the system analyzes the temperature stabilization filter contents for each temperature sensor. Sensors that exhibit large fluctuations in temperature response are marked bad and disregarded in further calibration. This type of error can be detected at room temperature and faulty sensors can be replaced before entering further calibration process.

2.10 Calibration error estimation − quality control

Total calibration error represents the main instrument for separation of faulty sensors. At the same time the calibration error relates directly to sensor quality and can provide means for sensor classification. The sensor signal conditioner uses digital representation of sensor characteristic described by equation (3). This description enables immediate evaluation of sensor properties, by running simulation algorithm of sensor response upon acquired calibration data. Total calibration error is calculated by simulating actual ASIC 16-bit arithmetic calculation, analyzed in equation (11).

At a first glance, the calibration error at every calibration point ε_{cpi} of the equation (11) should always yield 0. The calibration coefficients are obtained by resolving a system of equations. Calibration error is caused form coefficient rounding to integer value and by 16-bit integer arithmetic in signal conditioner. Calibration error value may differ ±1 LSB at every calibration point. Cumulative (RSS) error of the sensor characteristic approximation error should be as close as possible to zero. Large calibration error ε_{cpi} evaluation of sensor solution error may have several different causes. The causes for large calibration errors are analyzed by the sensor failure analysis software.

3. Results

Presented results are based on 34422 calibrated manifold absolute pressure sensors. Sensor properties investigation is presented on ZMD31020 signal.
In order to evaluate the input properties of uncalibrated sensors a histogram was plotted. The input temperature coefficient of pressure sensitivity at calibration point 3 in Fig. 1 is in the range of [-8%…-0.2%], which represents a insurmountable span of temperature coefficients, if analog calibration was to be made upon such sensors.

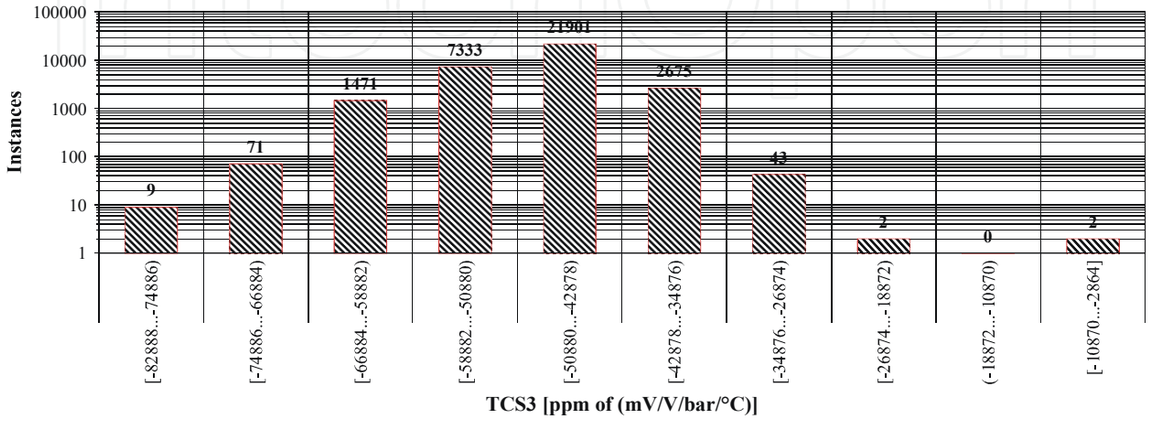

Fig. 5. Input temperature coefficient of sensitivity

Average value of input temperature coefficient of pressure sensitivity in the histogram, depicted in the Fig. 5 is -4.9% (mV/V/bar). Standard deviation from this value is 0.51% of (mV/V/bar). Sensors, based on analog signal conditioners with operational amplifiers (Schnatz et al., 1992), can compensate temperature coefficient of sensitivity up to 0.2%/°C. The latter demonstrates the advantage of the digital temperature compensation based signal conditioners. Input temperature coefficient of offset voltage is depicted in Fig. 6. Again, the plotted histogram depicts large variations for temperature coefficient of offset voltage. Analog calibration system could not calibrate the sensor with temperature coefficient of offset voltage in the range of 1mV/°C.

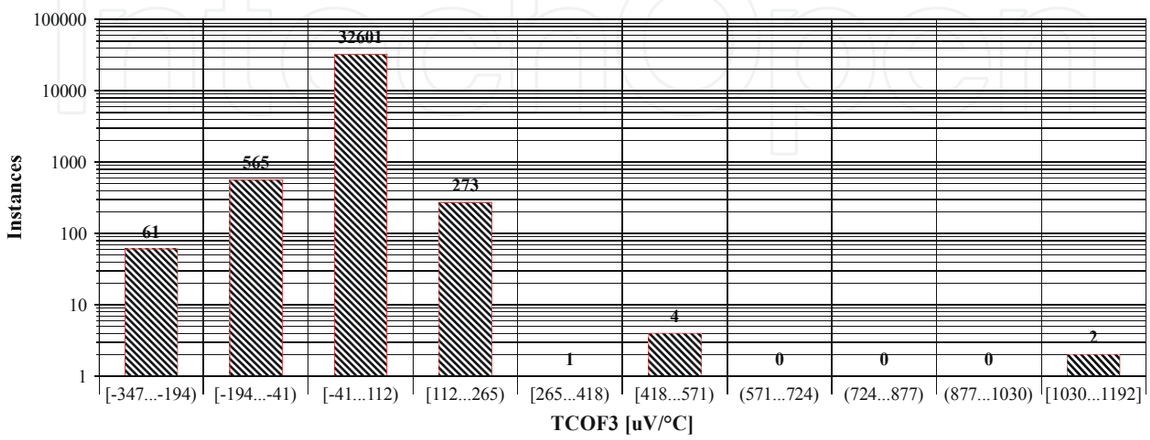

Fig. 6. Input temperature coefficient of offset voltage

In case of calibration of ZMD31020 based MAP sensors, further 11 test points were introduced to calibration scenario. Output temperature error histograms were evaluated at 5%, 10%, 20%, 30%, 40%, 50%, 60%, 70%, 80% and 90% of power supply voltage pressure response at 85°C and 20°C upon a set of 5828 sensors. From initial 5828 sensors, 366 were evaluated as bad. Among them were 182 sensors, lacking the results from testing at 20°C. Calculated histograms are a clear demonstration of effectiveness of digital temperature compensation. The histogram in Fig. 7 depicts the magnitude of temperature error in test point 1 (T=85°C, P=17kPa, V_{OUT}=5%V_{CC}). Presented result was subtracted with an ideal value and the resulting error was normalized in ppm. The data in the Fig. 7 shows temperature error in the range of [-0.2% … 0.38%] for 5075 sensors out of 5462 total, whereas the admissible range of temperature errors lies within ±1.7%.

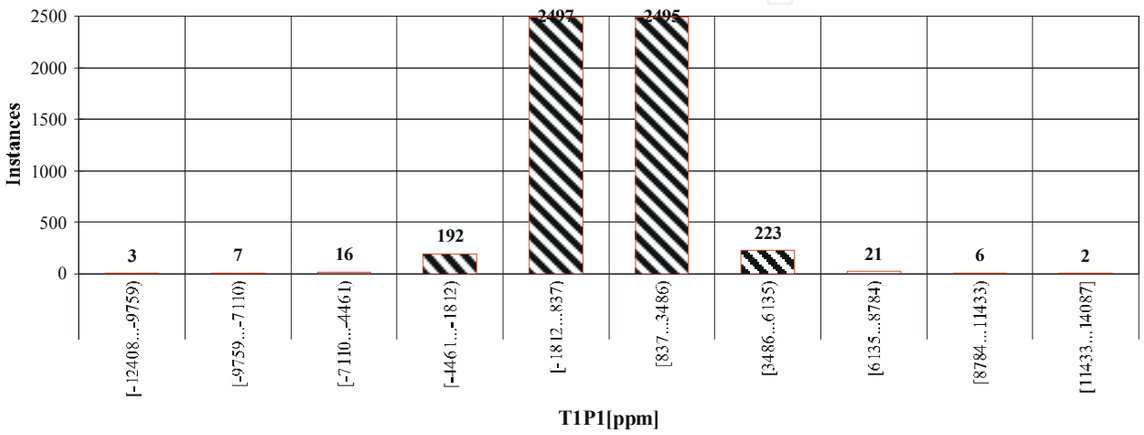

Fig. 7. Temperature error at test point 1

Mean histogram value, representing a typical calibration temperature error is 0.086%. The standard deviation from this value is 0.16%. Similar histogram was evaluated at test point 11 (T=20°C, P=105kPa, V_{OUT}=95%V_{CC}) and the resulting temperature error is depicted in Fig. 8. Mean histogram value is now 0.15%, while the standard deviance is 0.19%.

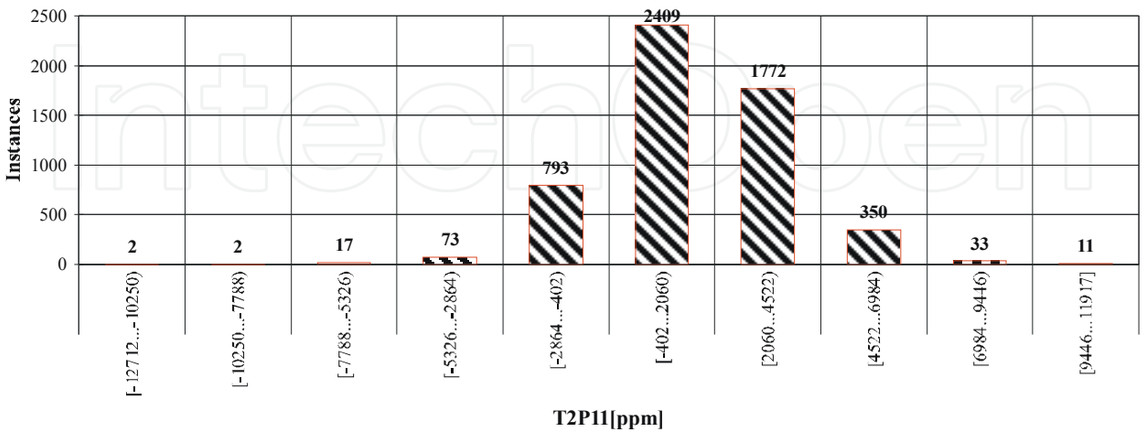

Fig. 8. Temperature error at test point 11

If remaining 184 sensors (366-182) bad sensors are further analyzed, the output stage failure is noted on 82 sensors, which can be attributed to faulty connection of the sensor output,

because the sensor output stays the same on every test point. The same cause of error can be attributed to faulty output stage – fault in signal conditioner. The actual cause can be determined with combined insight into calibration database. Remaining 102 sensors were calibrated with temperature error out of MAP sensor specification. One of them (ID=58800) was rejected by calibration process due to inadequate pressure response. Upon analysis of calibration database upon these 101 sensors, it becomes apparent that most of the tested sensors passed the calibration, but failed the test. The analysis of maximal sensor temperature error was performed on all tested temperatures. Resulting maximal errors were divided into 10 bins and the result was evaluated in the histogram. Resulting histogram is summarized in Table 1. The histogram depicts sensor classification in ten classes. The majority (5189 of 5462) of sensors are well within 0.7% limit of temperature error. Important is, that classification can be performed on each and every calibrated sensor. Because of complete sensor traceability, we are able to identify the class and quality for each calibrated sensor. The calibration yield upon 5462 sensors is 98.1%.

Class	Limit (ppm)		Sensors
	upper	lower	
1	767	2239	992
2	2239	3711	2190
3	3711	5183	1477
4	5183	6655	530
5	6655	8127	182
6	8127	9599	44
7	9599	11071	24
8	11071	12543	16
9	12543	14015	4
10	14015	15490	3

Table 1. Classification of calibrated sensors

The cause of failed sensors is attributed to change of sensor properties after calibration during packaging process. This was counter measured by performing the packaging process prior to calibration and performing the calibration as a last step of production process.

The adaptivity of the calibration system is based upon determining the limits of all system parameters, which define the criteria for quality of calibrated sensors. The result from criteria adaptation is the calibration interval for a given sensor property, based on sensors which comply with predefined output response. The limit optimization process is performed upon every sensor that enters the calibration process. Primary acquired sensor parameters are obtained directly from acquisition – raw pressure and temperature sensor readouts. The raw values are recalculated to analog measured quantity according to preamplifier settings, including sensor offset compensation and preamplifier gain.

An illustrative case of sensor limit adaptation is presented when a new sensor enter the calibration process. After initial acquisition of raw values the new sensor response is evaluated and its response is inserted in the histogram, which depicts the raw sensor readouts at the first calibration point (17kPa, -20°C). Entering sensor was assigned identification number (ID=31326).

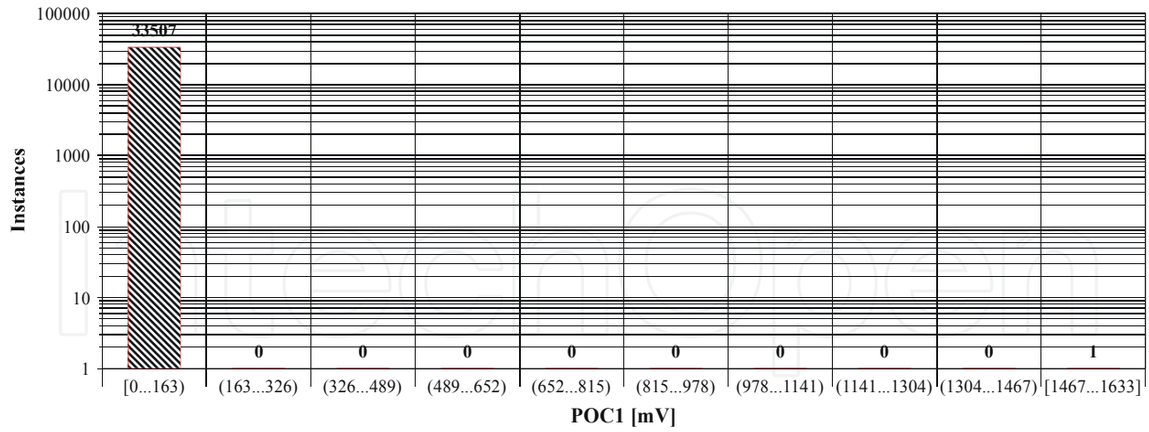

Fig. 9. Raw pressure sensor response at calibration point 1

From the histogram on Fig. 9, it is obvious, that the tested sensor extremely deviates in raw response from all other sensors. However, an automated analysis must establish other sensor properties in order to determine whether a given sensor will enter a full calibration process or not. Sole evaluation of the magnitude of raw pressure response is not sufficient for final estimation, because the sensors at the input can be e.g. from different manufacturers and their responses may vary. The calibration system is designed to adapt also to new type of sensor with different input properties. If several pressure points are scanned, the sensor properties can be evaluated (sensitivity, offset and nonlinearity). First, the sensor sensitivity is calculated as a difference of two pressure responses. If the sensor readout is approximately ten times larger than normal, then the sensitivity should be in proportion with raw readouts. Otherwise, the sensor response can be considered inadequate – this indicates failure in offset or gain optimization process. The system calculates the sensor sensitivity and depicts the result in the histogram for comparison with other sensors. The resulting histogram is depicted in the Fig. 10. The sensitivity was evaluated in the range between 300 and 338, which is in proportion with sensor readouts.

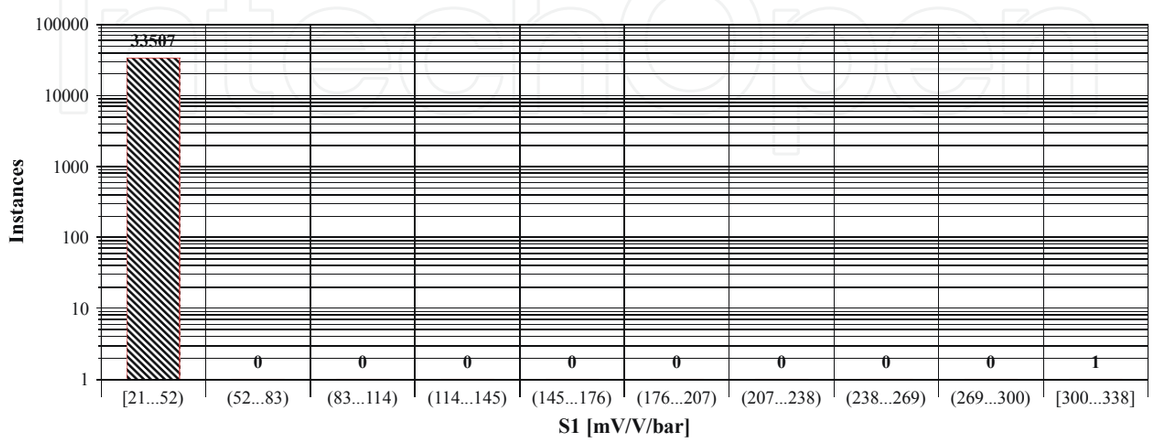

Fig. 10. Sensitivity at calibration point 1

Therefore, further analysis is performed and sensor nonlinearity is evaluated and the results are depicted in the Fig. 11. When the sensor nonlinearity is compared to other sensors in histogram, it becomes obvious, that the sensor is highly nonlinear (55.8%). Therefore, the sensor is discarded from further calibration process.

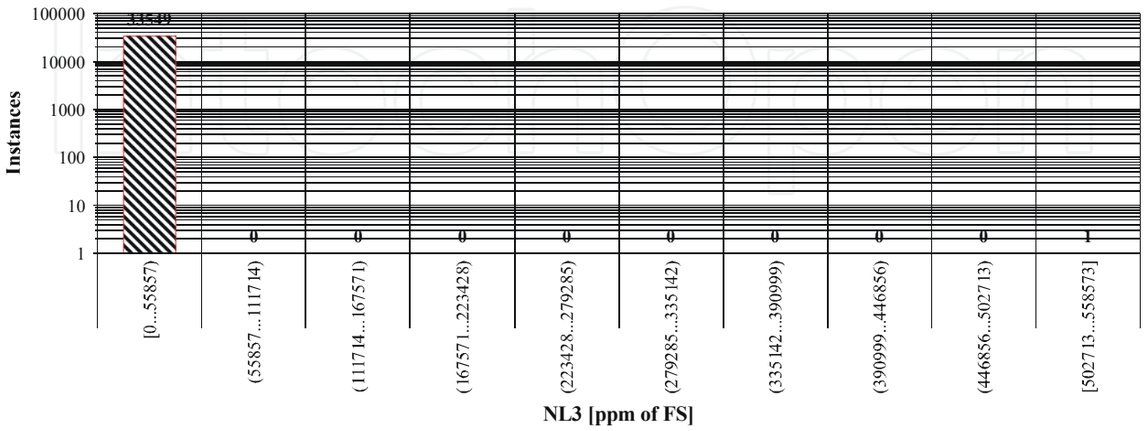

Fig. 11. Nonlinearity at calibration point 1

The sequence of high sensitivity and excess nonlinearity failures implies that a pressure sensor was not designed for calibration on a high pressure range: A low pressure sensor was exhibited to calibration on a high pressure range. Such a low pressure sensor exhibits larger sensitivity but also nonlinear response, when exposed to overpressure. Sensors such with nonlinearity can be calibrated, but not with the seven point calibration scenario, which was used during calibration process of manifold absolute pressure sensor.

Maximal nonlinearity of uncalibrated pressure sensors was limited to 2%. Sensor is discarded from further calibration and resulting histograms of raw pressure readout are evaluated again. Resulting histograms after discarding are depicted in Fig. 12 and Fig. 13.

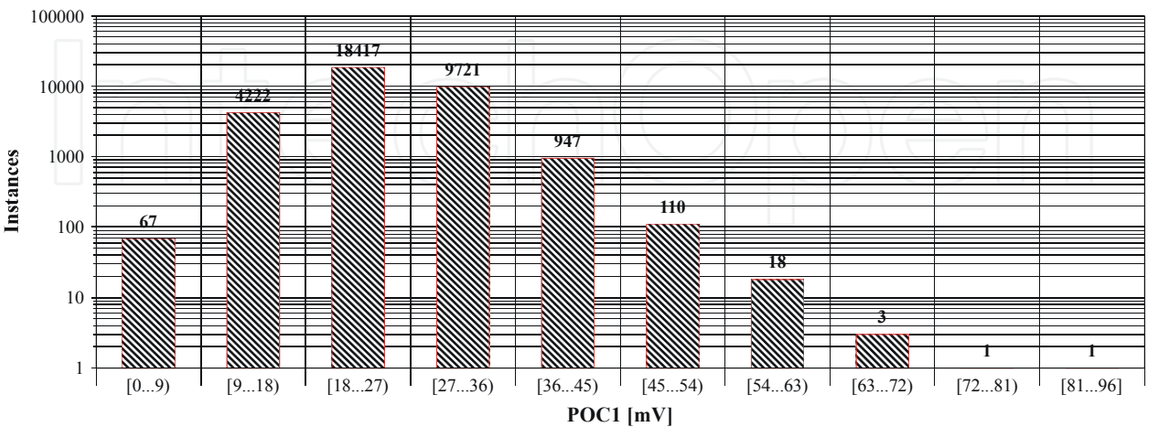

Fig. 12. Corrected raw pressure sensor response at calibration point 1

The resulting limits for raw pressure response stay between 0 and 96mV as can be seen in the Fig. 13, and for the pressure sensitivity in interval [21…41mV/V/bar].

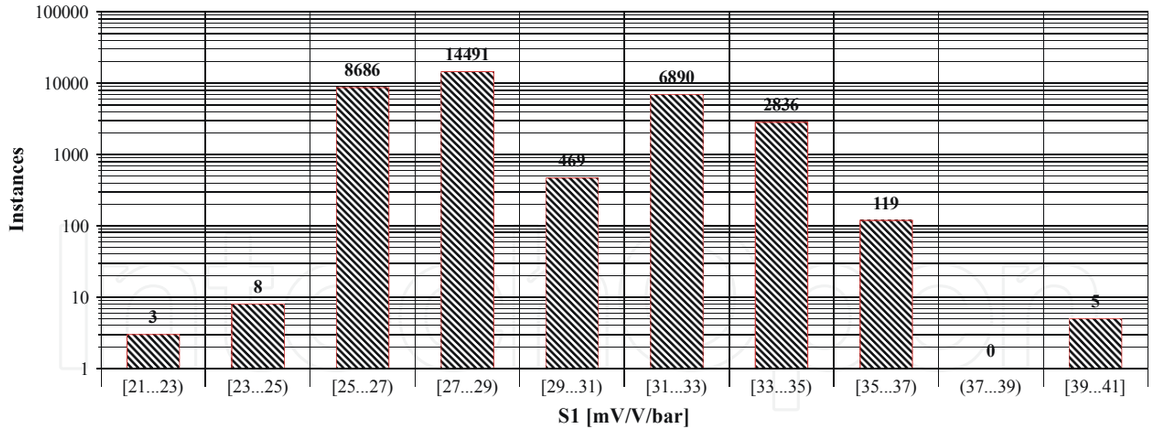

Fig. 13. Corrected pressure sensor sensitivity at calibration point 1

Failure analysis was performed upon a set of calibrated sensors. A detailed insight of failure analysis results is summarized in Table 2. Calibration yield, which would be calculated disregarding failure analysis, would yield 93.7%, since there are 2289 failed sensor out of 36711 calibrated. However, the calibration database stores everything including failed attempts related to system causes, which are not caused by failed sensors. Most of system failures are attributed to improper sensor connection (operator error). Therefore the system related causes must be removed from analysis to obtain actual yield of calibration. After this, the calibration yield improves to 96.8%, since there are only 1127 failed sensors of 35549.

Cause of failure	Origin of failure	Nr. of sensors
Inadequate response of pressure sensor	Sensor	220
Inadequate response of temperature sensor	Conditioner	81
Calibration coefficients clamped	Calibration	373
Communication failure	System	1108
Inadequate temperature stabilization	System	34
Excess nonlinearity	Sensor	384
Tolerance error during coefficient calculation	Calibration	36
Calibration of sensor output stage failure	System	20
Output stage clamped to maximum level	Conditioner	33
Total		2289

Table 2. Failure analysis of calibrated sensors

4. Conclusions

Adaptive calibration and quality control were presented. During initial calibration stage early detection of faulty sensors has proven essential for calibration system yield improvement. Yield enhancement is achieved by thorough specification of sensor related failure causes. Further refinement of calibration failure causes gives a detailed insight into sensor related failures by thorough evaluation of essential sensor properties such as nonlinearity, offset and sensitivity. Described quality control mechanisms enable automatic sensor classification. Proposed calibration system shortens the total time for calibration of

smart sensors by implementing the input testing of the sensor parameters as well as final testing of the calibrated sensors. Final testing was achieved by inserting excess test points into the calibration scenario. In its maximal extension, which offers calibration of 2048 sensors at a time, the calibration time was reduced to 3 seconds per sensor – in its current configuration, the total calibration time is 42 seconds per sensor.

5. References

International technology roadmap for semiconductors. 2006 update - Test And Test Equipment Electronic file available at: http://www.itrs.net/Links/2006Update/FinalToPost/03_Test2006Update.pdf, 2008

International technology roadmap for semiconductors. 2006 update - Yield Enhancement Electronic file available at: http://www.itrs.net/Links/2006Update/FinalToPost/13_Yield2006Update.pdf, 2008

Takashima, Y.; Adachi, T. & Yoshino, T. & Yamada, T. (1997). Temperature compensation method for piezoresistive sensors. *JSAE Review*, Volume 18, Issue 3 (1997), pp. 317 319

IEEE Std. 1451.2 D3.05-Aug1997. IEEE standard for a smart transducer interface for sensors and actuators – Transducer to microprocessor communication protocols and transducer electronic data sheet (TEDS) formats. Institute of Electrical and Electronics Engineers, September 1997

Chau, M.; Dominguez, D. & Bonvalot, B. & Suski, J. (1997). CMOS fully digital integrated pressure sensors. Sensors and Actuators A, Volume 60, Issues 1-3 (1997), pp. 86 89

Wang, Q.; Ding, J. & Wang, W. (2005). Fabrication and temperature coefficient compensation technology of low cost high temperature pressure sensor. *Sensors and Actuators A*, Volume 120, Issue 2 (2005) 468 473

Schnatz, F. V. et al. (1992). Smart CMOS capacitive pressure transducer with on-chip calibration capability. *Sensors and Actuators A*, Volume 34, Issue 1 (1992), pp. 77 83

Lee, Bo-Na et al. (1999). Calibration and temperature compensation of silicon pressure sensors using ion-implanted trimming resistors. *Sensors and Actuators A*, Volume 72 (1999), pp. 148 152

ZMD31020 Advanced Differential Sensor Signal Conditioner Functional Description Rev. 0.75, (2002) ZMD AG

ZMD31050 Advanced Differential Sensor Signal Conditioner Functional Description Rev. 0.75, (2005), ZMD AG

MLX90269 Absolute Integrated Pressure Sensor datasheet, June 2006, *Melexis- Microelectronic Integrated Systems Inc., rev 2*

Možek, M.; Vrtačnik, D. & Resnik, D. & Aljančič, U. & Penič, S. & Amon, S. (2008). Digital self-learning calibration system for smart sensors. *Sensors and Actuators A*. 141 (2008), 141, pp. 101 108

Applications and Experiences of Quality Control
Edited by Prof. Ognyan Ivanov

ISBN 978-953-307-236-4
Hard cover, 704 pages
Publisher InTech
Published online 26, April, 2011
Published in print edition April, 2011

The rich palette of topics set out in this book provides a sufficiently broad overview of the developments in the field of quality control. By providing detailed information on various aspects of quality control, this book can serve as a basis for starting interdisciplinary cooperation, which has increasingly become an integral part of scientific and applied research.

How to reference
In order to correctly reference this scholarly work, feel free to copy and paste the following:

Matej Možek, Danilo Vrtačnik, Drago Resnik, Borut Pečar and Slavko Amon (2011). Adaptive Calibration and Quality Control of Smart Sensors, Applications and Experiences of Quality Control, Prof. Ognyan Ivanov (Ed.), ISBN: 978-953-307-236-4, InTech, Available from: http://www.intechopen.com/books/applications-and-experiences-of-quality-control/adaptive-calibration-and-quality-control-of-smart-sensors

INTECH
open science | open minds

InTech Europe
University Campus STeP Ri
Slavka Krautzeka 83/A
51000 Rijeka, Croatia
Phone: +385 (51) 770 447
Fax: +385 (51) 686 166
www.intechopen.com

InTech China
Unit 405, Office Block, Hotel Equatorial Shanghai
No.65, Yan An Road (West), Shanghai, 200040, China
中国上海市延安西路65号上海国际贵都大饭店办公楼405单元
Phone: +86-21-62489820
Fax: +86-21-62489821

IntechOpen